Fifth International Conference on CFD in the Process Industries
CSIRO, Melbourne, Australia
13-15 December 2006

CFD MODELLING FOR AN ENTRAINED FLOW GASIFICATION REACTOR USING MEASURED "INTRINSIC" KINETIC DATA

San Shwe HLA, D.J. HARRIS and D.G. ROBERTS

CRC for Coal in Sustainable Development
CSIRO Energy Technology
PO Box 883 Kenmore, QLD 4069, AUSTRALIA
san.hla@csiro.au

ABSTRACT

Intrinsic (chemical) kinetic data for gas-char reactions are typically measured under conditions where temperatures and pressures are lower than those in operational entrained flow gasifiers/combustors. In this paper, a method using an "effectiveness factor" is applied to use intrinsic data in the determination of gasification rates at high temperatures and pressures as a function of several parameters (physical and morphological properties of coal-char and reactor conditions). A sub-model for gas-char reactions has been written and linked with a commercial CFD package, *FLUENT,* as a user-defined function (*UDF*).

The numerical model presented in this paper is a steady-state 2D axial-symmetric model which also includes coal devolatilisation, volatiles gas combustion; the effects of turbulence on the motion of the coal particles; and radiative heat transfer in the gas phase, moving particles and reactor walls. A Lagrangian scheme is used to trace the particles.

The model provides detailed information on temperatures, reaction rates, gas composition and carbon conversion along the length of a high pressure entrained-flow reactor. A series of numerical simulations has been performed for the gasification of a range of Australian bituminous coals under different operating conditions (reactor temperatures & O:C ratio), and the results are then compared with the experimental data. The model results are consistent with operating practice, and provide novel insights into our understanding of the coal gasification reaction system.

Keywords: High Temperature Reactivity, Entrained Flow Reactor, CFD

NOMENCLATURE

A_e external surface area of char particle (m^2/g)
A_i frequency factor of reaction ($kg.m^{-2}.s^{-1}.[atm]^{-n}$)
A_{total} specific total surface area of char particle (m^2/g)
d particle diameter (m)
D_e effective diffusion coefficient (m^2/s)
E_i activation energy of gas-char reaction (kJ/kmol)
k_i intrinsic rate coefficient on area basis ($kg.m^{-2}.s^{-1}.[atm]^{-n}$)
k_d Gas Film diffusion coefficient (m/s)
M_C molecular weight of carbon (kg/kmol)
n reaction order (-)
P_{gi} gaseous component pressure at main stream (atm)
P_{si} gaseous component pressure at particle surface (atm)
R_i rate of reaction (kg/kg/s)
R universal gas constant (kJ/kmol/K)
T temperature (K)
η effectiveness factor (-)
ϕ Thiele modulus (-)
ρ apparent density of char (kg/m^3)
υ_g stoichiometric coefficient (-)
$_i$ gas char reaction (or) reactants, O_2, CO_2, H_2O, H_2

INTRODUCTION

Integrated gasification combined cycle (IGCC) power generation systems are considered as prospective next-generation technology for power generation from coal providing attractive options for reduction in CO_2 emissions and other environmental issues associated with gaseous and solid emissions from power systems. One of the key enabling technologies fundamental to any IGCC system is the gasification process, which is largely influenced by coal type and operating conditions. It is essential that the behaviour of Australian coals in these new gasification technologies is fully understood in order to assist power utilities in their adoption of the new technologies, and to help coal exporters to market Australian coals overseas.

Mathematical modelling of the gasifier is an important component in the evaluation of operability studies on a combined cycle power generation scheme. Over the last few decades, CFD modelling coupled with a detailed understanding of the coal combustion process has been a key tool in improving the performance of traditional pulverised coal fired systems. Likewise, CFD modelling can be used as a tool to provide insights into the flow field within the gasifier that will lead to improved performance.

The modelling of gasification of different types of coal requires a detailed understanding of the coal and char reactions under gasifier conditions. To investigate the performance of Australian coals under high pressures and temperatures, an experimental program is underway based on a pressurised entrained-flow reactor (*PEFR*) (Harris, Roberts and Henderson, 2006) and associated laboratory scale facilities (Roberts and Harris, 2000).

The purpose of the present simulation is to develop and analyse a mathematical model for interpretation and application of measured intrinsic gasification kinetic data to an experimental reactor which operates under more complex reacting conditions.

MODEL DESCRIPTION

A generalised finite volume method (Patankar, 1980) based CFD code, *FLUENT*, is utilised to model the *PEFR*. The model includes following physical and chemical processes:

- fluid phase turbulent flow and mixing of gaseous reactants
- turbulent dispersion of coal particles
- convective and radiative heat transfer among solid phase, gas phase and reactor walls
- coal devolatilisation
- volatiles and combustible gases oxidation
- heterogeneous gas-char reactions
- homogeneous water-gas shift reaction

Due to their complexities, sub-models to determine the reaction rates for gas-char reactions and water-gas shift reaction are separately developed and exported to *FLUENT* as user-defined functions (*UDFs*). Other processes are modelled using sub-models readily available in *FLUENT*.

Mechanism for heterogeneous gas-char reaction

Estimation of heterogeneous reaction rates is critical for gasification processes as their relative slowness controls the conversion level and gas composition of any gasifiers. In this model, four reactants (O_2, CO_2, H_2O and H_2) are considered for reaction with char and an empirical nth order rate equation with an effectiveness factor (Eq. 1) is used to calculate conversion rates at elevated pressures and temperatures (Laurendeau, 1978).

$$R_i = \eta A_{total} A_i P_{Si}^n e^{-E_i/RT} \tag{1}$$

The effectiveness factor, η, is used to model the extent to which chemical reaction rates are affected by diffusion through char pores. The effectiveness factor and partial pressure of the reactant, P_{si}, are two key parameters involved in Eq.1. The effectiveness factor is usually expressed as a function of the Thiele modulus (Eq. 2) for spherical-shaped particles.

$$\eta = \frac{3}{\phi}\left(\frac{1}{\tanh(\phi)} - \frac{1}{\phi}\right) \tag{2}$$

An equation for a generalised Thiele modulus is derived from a published review (Laurendeau, 1978) to allow for calculation of the modulus for reactions with any reaction order.

$$\phi = \frac{d}{6}\left(\frac{(n+1)k_i \rho \upsilon_g A_{total} R T_g P_{Si}^n}{2 M_C D_e P_{Si}^n}\right)^{\frac{1}{2}} \tag{3}$$

The partial pressure of reactant at the particle surface is unknown, but can be estimated using the bulk diffusion rate as:

$$P_{Si} = P_{gi} - \frac{R_i}{K_d A_e} \tag{4}$$

Solving for partial pressure of reactant at the particle surface is not straightforward. From equation 1 to 4, it can be seen that the overall reaction rate is a function of P_{Si}, which can not be estimated without knowing the overall reaction rate. By combining equations 1 and 4, unknown P_{Si} can be found using a suitable iterative procedure. In this study, Brent's method (Brent, 1971) is used for solving this problem.

It is clear from equation (1) that total char surface area, A_{total}, is an important parameter in determining the rate of heterogeneous reactions. Char surface area changes with level of char burn off, char type, and prevailing reaction conditions, making it extremely difficult to model and predict. A greater understanding of these phenomena is required; however, for the present purpose, surface area at different levels of carbon conversion is estimated using a method described by discrete random pore model (Bhatia and Vartak, 1996). Input parameters required to this sub-model has been determined using measured surface area data of char samples taken from PEFR experiments at various extents of conversion (Harris, Kelly and Roberts, 2002). Detailed information of properties of coal and intrinsic reactivity data such as frequency factors, activation energies and reaction orders used in this model can be found in Hla, Harris and Roberts (2005).

Sub-models

The basic transport equations governing turbulent flow are derived from the laws of conservation of mass, momentum and energy. Turbulence in the gas phase was modelled by the two equation realizable k-ε model for closure (Shih *et al.*, 1995). On the other hand, particle dispersion modelling describes how particles respond to viscous forces from turbulent flow. This sub-model is based on the discrete random-walk simulations in a Lagrangian coordinate, which are thought to be the most accurate for the dilute suspensions (Shuen, Chen and Feath, 1983). The effect of radiation heat transfer to the particles is included by using discrete ordinates (DO) radiation model (Chui and Raithby, 1993; Raithby and Chui, 1990).

When coal particles enter a high temperature system, they immediately and rapidly release volatiles before the resultant coal char undergoes (relatively slow) heterogeneous combustion and gasification. In this simulation, a two-step devolatilisation model is used for the rate of volatile released (Kobayashi, Howard and Sarofim, 1977). The gas phase is modelled as a multi-component mixture, including N_2, O_2, H_2O, CO, CO_2, CH_4 and CH_xO_y (a general oxygenate that is the gaseous outcome of the particle pyrolysis). These components are accounted for by means of their mass fractions of volatile yield. CO and H_2 resulting from gasification reactions are incorporated to the gas phase, and if stoichiometric conditions allow them, they are oxidised to CO_2 and H_2O respectively, by means of homogenous reactions. For gas combustion reactions, both turbulent mixing and finite chemical reaction rates are considered. These two reaction rates are compared in the computational solution process, and the slower of them is taken to represent the effective controlling rate. Water-gas shift reaction ($CO+H_2O \leftrightarrow CO_2+H_2$) is considered as another gas phase reaction in this model. This reaction is assumed to proceed to chemical equilibrium at all locations inside the reactor and calculation for forward and backward reaction rate using equilibrium constant is extracted from previous published simulation works (Liu, Zhang and Park, 2001; Wen and Chaung, 1979). This assumption is supported by experimental work using this reactor (Harris, Roberts and Henderson, 2006).

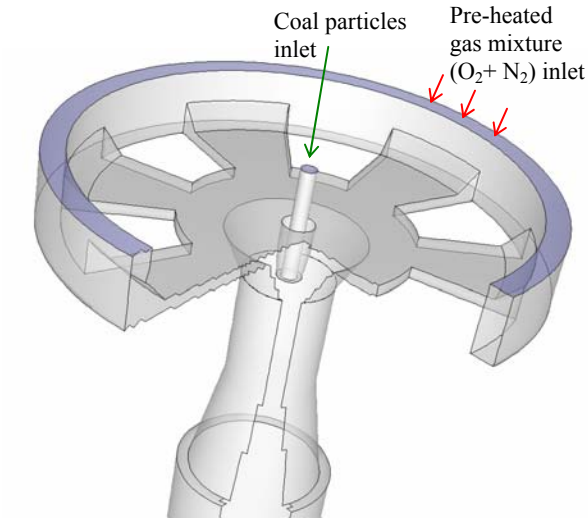

Figure 1: Schematic diagram of reactor inlet system

Pressurised entrained-flow reactor

The *PEFR* is a facility designed to allow investigation of high pressure gasification processes under conditions where key conversion phenomena can be isolated and studied. The coal and gas inlet system of *PEFR* is shown in Figure 1.

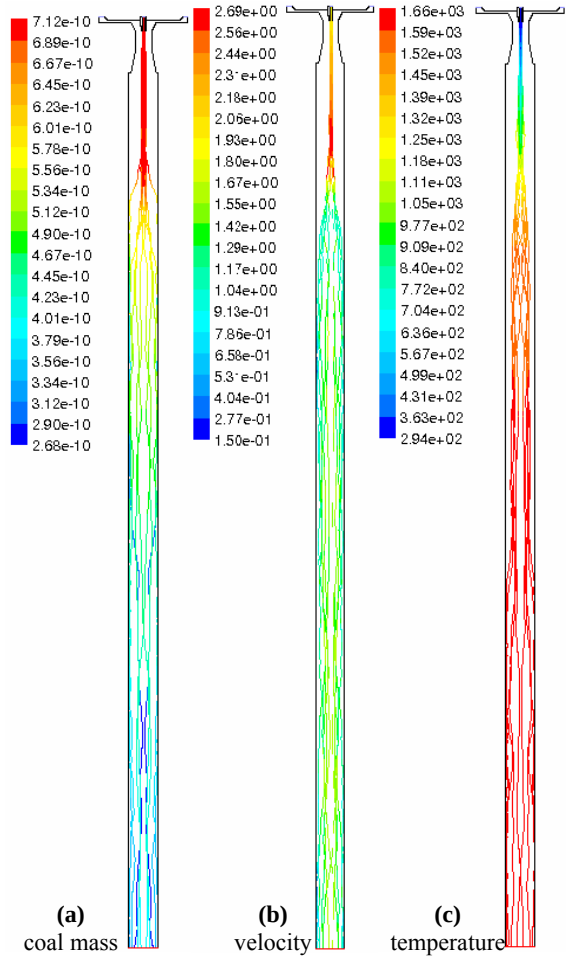

Figure 2: Coal particle trajectories

The coal particles are injected into the reactor along with some inert gas (N_2) through the central nozzle while diluted O_2 is blown in through six channels at the sides. For the simplicity of simulation, these six channels are considered as an equivalent annulus so that this three-dimensional geometry can be reduced to a two-dimensional axial-symmetric case.

Typically, the gas enters the axial inlets through the rim with a speed of 0.4 m/s (Figure 1). The coal particles enter through a nozzle along with inert N_2 gas with a superficial velocity about 1.8 m/s. Coal devolatilisation, combustion and gasification occurs in a 70 mm internal diameter and 2100 mm long heated tube. The reactor is operated at pressure of 20 bar, a range of (controlled) wall temperatures (1100°C -1400°C) and a range of O:C ratios (60%-200%). The feed coal and carrier gas (N_2) temperatures are around ambient and the diluted oxygen is pre-heated to a temperature of ~900°C. Details of the reactor design and additional background can be found in elsewhere (Harris, Roberts and Henderson, 2006). Uniform distributions of inlet velocity and temperature, fully developed flow conditions at the outlet, and no slip conditions at the wall are defined in the model.

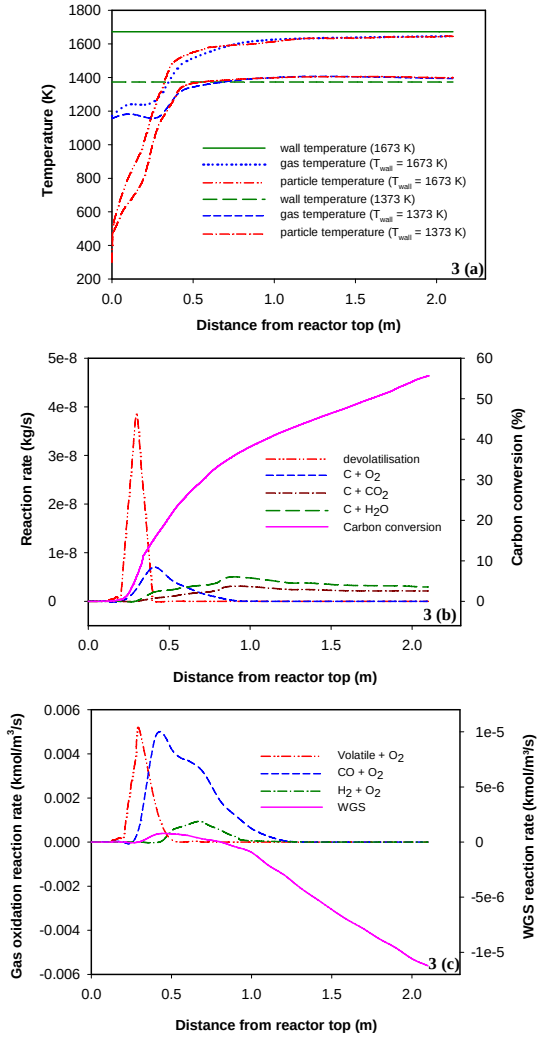

Figure 3: Profile of (a) temperature, (b) gas-char reaction rates [reactor wall temperature= 1673K], (c) homogeneous reaction rates [reactor wall temperature= 1673K]

MODEL RESULTS AND COMPARISONS

Figure 2 shows coal particle trajectories, coloured by coal mass, particle velocity and particle temperature, reflecting a typical experimental run for an Australian reference coal. When coal enters the reactor and is quickly heated and devolatilises. The coal particles rapidly form char, partially oxidise, and the remainder is consumed by the relatively slow gasification reactions. At the entrance of the reactor, the particle velocity is the same as inlet velocity (1.8m/s). It then increases due to velocity increase of inert carrier as it mixes with preheated gas. When the gas mixture flow develops well inside the reactor tube, the coal particles are entrained with the whole gas mixture and its velocity reduces to gas mixture velocities (average value is about 1.1 m/s) along the remaining length of the reactor. Unlike the practical gasifier, the main heat source of the reactor is coming from external heating elements; it can be seen in Figure 4(a) that gases near reactor walls are heated faster than those close to the centre.

In Figure 3(a), area-weighted average values of gas and coal particles temperature for two different reactor wall temperatures are also presented. Model results show that the particle temperature increases rapidly at the entrance of the reactor. This is due to heat transfer from both reactor wall and preheated gas phase. As expected, both solid and gas phase temperatures increase when oxidation of the volatiles and char takes place. It is observed that significant difference between gas and particle temperatures disappears 500 mm below the gas and coal particles inlet point for both cases. It is interesting that, for the case of lower reactor wall temperature (1100°C), gas and coal temperatures reach the wall temperature around 600 mm below the inlet point while for the case of higher reactor wall temperature (1400°C), gas and solid temperatures do not attain the wall temperature even at the reactor exit point.

Figure 3(b) presents the profile of devolatilisation and gas-char reactions together with the carbon conversion. As the figure shows, devolatilisation starts very rapidly and is completed within 400 mm below the reactor top which corresponds to a residence time of 0.2 sec. Char oxidation starts when pyrolysis rate reaches a maximum and occurs over a greater distance and time than the devolatilisation process. Char gasification reactions occur simultaneously with oxidation and their rates are greatest around the point where oxidation is completed and decrease steadily while carbon conversion increases. The carbon conversion plot (Fig. 3(b)) can be divided into two parts, each with a different gradient: the first rapid increase is largely attributable to devolatilisation and char combustion process; the second more steady conversion stage is associated with char gasification reactions. Figure 3(c) shows homogeneous gas reaction rates along the reactor. As expected, volatile oxidation starts just below the point where volatile gases are released, followed by CO and H_2 oxidation reactions. CO reaction rates are markedly higher since the amount of CO released by char combustion processes is significantly higher than the amounts of H_2 released by steam gasification reaction. Forward water-gas-shift reaction occurs along the first 1000 mm of the reactor when average gas temperature is relatively low and, backward reaction takes place for the remaining length of the reactor.

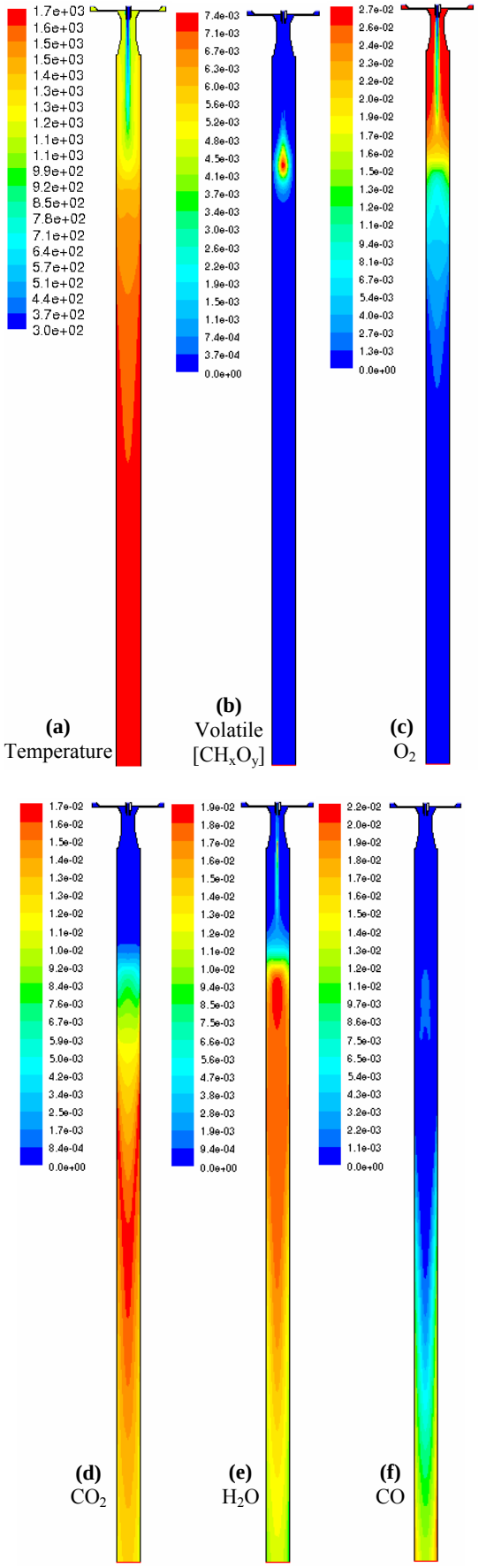

Figure 4: Contour of gas temperature in K and gas composition in molar fraction

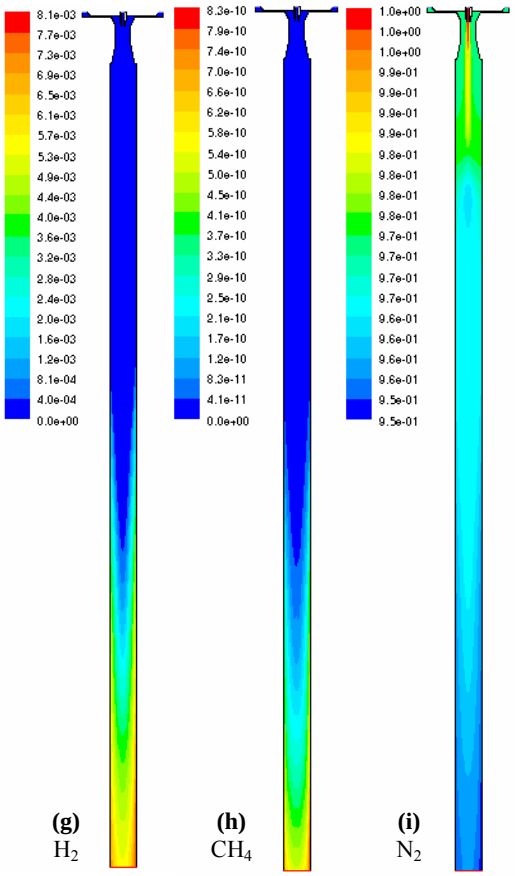

Figure 4 (Continue): Contour of gas temperature in K and gas composition in molar fraction

Figure 4 shows the simulated axial and radial distributions of the gas temperature and gas composition which represent a typical *PEFR* experimental run using the reference coal. Volatiles are released while coal particles are mainly entrained by the carrier gas before this inert gas fully mixes with inlet gas mixture. Therefore, volatile gas are mainly released and consumed at the centre within the top 400mm of the reactor (see Figure 4(b)). In the first 250mm of the reactor, oxygen is available in the peripheral annulus of the flow before it diffuses and mixes with inert gas. As O_2 moves further into the gasifier, more and more is consumed by volatile and char combustion and eventually no O_2 remains in the lower section (1000 mm below the reactor top).

During the initial combustion stage (while O_2 is present), even though the gasification reactions occur (as discussed above), any hydrogen or carbon monoxide produced is immediately consumed in the gas phase so that only a very small amount of CO is observed within char combustion zone (Figure 4 (f)). Only when the oxygen concentration falls to zero do hydrogen and carbon monoxide appear in the bulk gas. CO and H_2 concentration then increase monotonically along the remaining length of gasifier to reach a maximum at the outlet. Contrary to CO and H_2, in the initial oxidation period the concentrations of steam and CO_2 increase, showing maxima just after the oxygen disappears and then decrease due to gasification reaction. Figure 4(e) shows that small fraction of steam is found at the central region of the reactor top due to moisture evaporation from the coal. The presence of only a very small quantity of methane reported in Figure 4(h) indicates that the kinetics of the hydro-gasification of coal could also be ignored under these conditions. For a clearer presentation of the behaviour of gas phase species formation and consumption inside the reactor, area-weighted gas composition profiles are plotted in Figure 5.

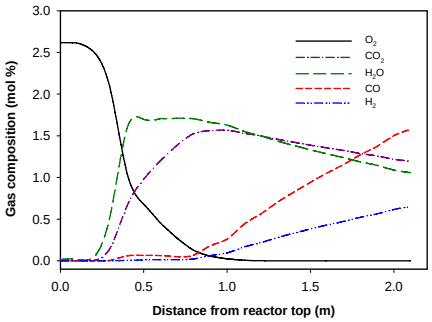

Figure 5: Gas composition profile

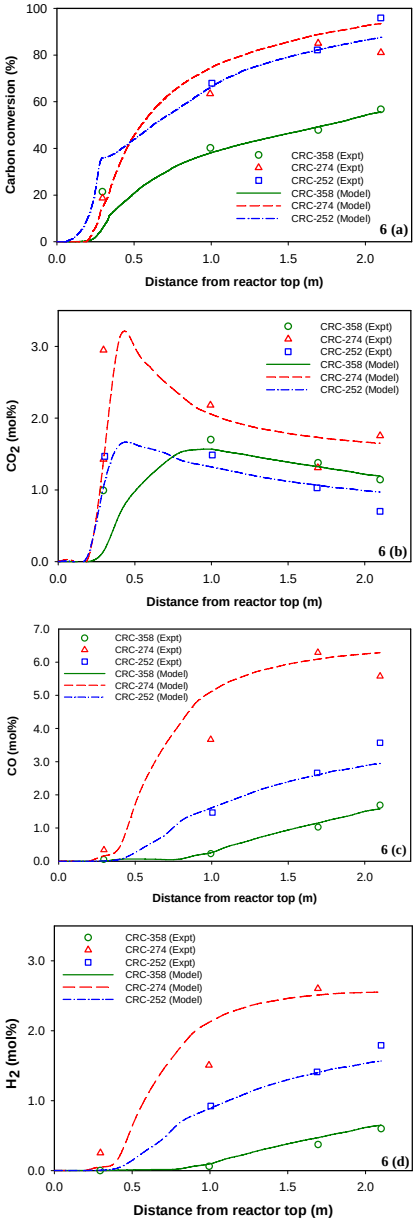

Figure 6: Comparison between model and experimental results [Reactor wall temperature = 1673K]

To verify the validity of the model, the simulation results are compared with the experimental data in two approaches; the first validation is done by comparing the profile of carbon conversion and gas composition; and the second approach compares reactor performance at the exit as a function of the molar O:C ratio for different Australian coals. Here, O:C ratio refers to the ratio of the theoretical O required for conversion of the C fed in the coal to CO. It can be seen in Figure 6(a) model calculations clearly differentiate between initial rapid devolatilisation/combustion processes and the slower char gasification. The significance of volatile yield on carbon conversion is demonstrated in Figure 6(a). This figure shows that similar gasification reaction rates are achieved for two of the three different coals (namely CRC-358 and CRC-252) but different levels of carbon conversion are observed at the initial stage of the reactor. Figure 6 shows that the model is able to predict well the profile of carbon conversion and gas composition for different types of Australian coals for which kinetic data are available. This demonstrates that it is possible to apply bench-scale 'intrinsic' reactivity data to interpretation of coal gasification behaviour under far more complex high pressure and high temperature conditions.

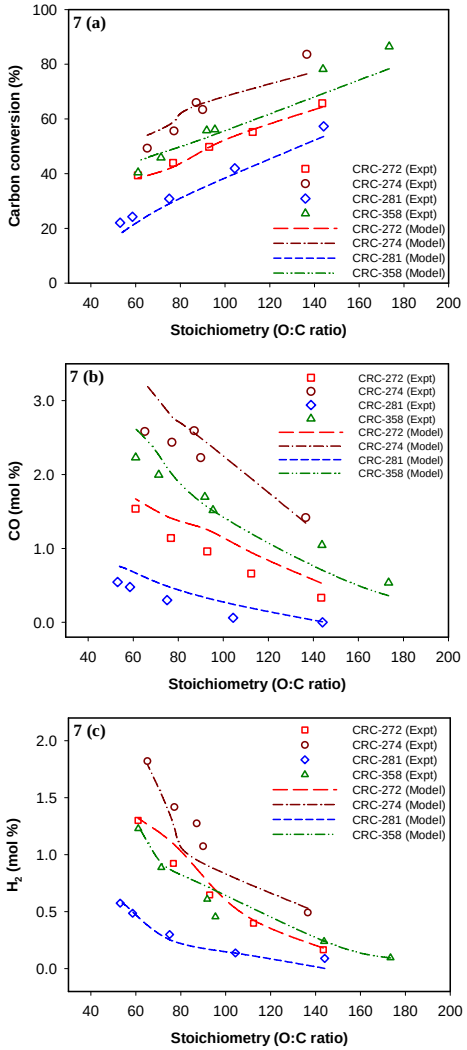

Figure 7: Comparison between model and experimental effects of O:C ratio on reactor performance [CRC-272 & CRC-281 for 1373 K reactor wall temperature, CRC-274 & CRC-358 for 1673 K reactor wall temperature]

In a short residence time reactor, like an entrained flow reactor/gasifier, the O:C ratio is critical to the conversion and gas composition since it determines the amount of H_2O and CO_2 released from char and volatile combustion. The concentrations of these species directly affect gasification reaction rates which control exit carbon conversion level and gas composition. The effect of the O:C ratio, in this study, is investigated by changing the coal feed rate while keeping other parameters unchanged.

Figure 7 shows the effect of the O:C ratio on the calculated and measured values of carbon conversions and gas composition. As expected, the calculated and measured carbon conversion increases when the O:C ratio increases. A greater O:C stoichiometry increases the rate of combustion simply because more oxygen is available to react with both char and volatile gases, and the gasification rate also increases since a greater amount of CO_2 and H_2O is released from the oxidation processes. Figure 7 shows that model calculations of gas phase concentrations for the different stoichiometry ranges agree well with the measured values, confirming that the gasification sub-models applied in this study provide a reasonable estimate of gas-char reaction rates at high pressure and high temperature.

CONCLUSIONS

The model shows that volatile matter is released and oxidised very quickly. Once oxygen levels are depleted, carbon monoxide and hydrogen concentrations increase over the remaining length of the reactor and it is found that gasification reactions of char mainly occur at temperatures close to the wall temperatures.

High volatile matter in coal results in high carbon conversion due to the rapid volatile release during initial stages of coal gasification. It is seen that a knowledge of the char reactivity and physical structure for each coal are essential to obtain a reasonable prediction of carbon conversion at high temperatures and pressures.

The simulation results are compared with the experimental data for a range of O:C ratios. It illustrates that the calculated carbon conversions and gas compositions agree well with the measured ones for several different Australian coals. Both experimental and model results show that the O:C ration has a significant influence on the product gas distribution. It is found that an increase in the O:C ratios decreases the H_2 and CO concentration.

The model's predictions are consistent with operating practice suggesting that the mechanism/submodels for gasification reactions used in this model are acceptable for future modelling work of pressurised entrained flow gasifiers using Australian coals as feedstocks.

ACKNOWLEDGMENTS

The authors wish to acknowledge the financial support provided by the Cooperative Research Centre for Coal in Sustainable Development, which is funded in part by the Cooperative Research Centres Program of the Commonwealth Government of Australia.

REFERENCES

BHATIA, S.K. and VARTAK, B.J., (1996), "Reaction of microporous solids: The discrete random pore model", *Carbon*, **34**(11), 1383-1391.

BRENT, R.P., (1971), "An algorithm with guaranteed convergence for finding a zero of a function", *The Computer Journal*, **14**(5), 422-425.

CHUI, E.H. and RAITHBY, G.D., (1993), "Computation of radiant heat transfer on a non-orthogonal mesh using the finite-volume method", *Numerical heat transfer, Part B*, **23**, 269-288.

HARRIS, D.J., KELLY, M.D. and ROBERTS, D.G., (2002), "Reactivity Characterisation of Australian Coals for use in Advanced Technologies", *CRC for Black Coal Utilisation Research Report 35*, CRC for Black Coal Utilisation.

HARRIS, D.J., ROBERTS, D.G. and HENDERSON, D.G., (2006), "Gasification behaviour of Australian coals at high temperature and pressure", *Fuel*, **85**(2), 134-142.

HLA, S.S., HARRIS, D.J. and ROBERTS, D.G., (2005), "A coal conversion model for interpretation and application of gasification reactivity data", *International Conference on Coal Science and Technology*, Okinawa, Japan.

KOBAYASHI, H., HOWARD, J.B. and SAROFIM, A.F., (1977), "Coal devolatilization at high temperatures", *18th Symposium (International) on Combustion*, 411.

LAURENDEAU, N.M., (1978), "Heterogeneous Kinetics of Coal Char Gasification and Combustion", *Progress in Energy and Combustion Science*, **4**, 221-270.

LIU, X.J., ZHANG, W.R. and PARK, T.J., (2001), "Modelling caol gasification in entrained flow gasifier", *Combustion Theory and Modelling*, **5**, 595-608.

PATANKAR, S.V., (1980), "Numerical heat transfer and fluid flow", McGraw-Hill, New York.

RAITHBY, G.D. and CHUI, E.H., (1990), "A finite-volume method for predicting a radiant heat transfer in enclosures with participating media." *J. Heat Transfer*, **112**, 415-423.

ROBERTS, D.G. and HARRIS, D.J., (2000), "Char Gasification with O_2, CO_2 and H_2O: Effects of Pressure on Intrinsic Reaction Kinetics", *Energy and Fuels*, **14**(2), 483-489.

SHIH, T.-H., LIOU, W.W., SHABBIR, A., YANG, Z. and ZHU, J., (1995), "A new k-e eddy-viscosity model for high Reynolds number turbulent flows- Model development and validation", *Computers Fluids*, **24**(3), 227-238.

SHUEN, J.S., CHEN, L.D. and FEATH, G.M., (1983), "Evaluation of a stochastic model of particle dispersion in a turbulent round jet", *A.I.Ch.E. Journal*, **29**, 167-170.

WEN, C.Y. and CHAUNG, T.Z., (1979), "Entrainment coal gasification modeling", *Ind. Eng. Chem. Process Des. Dev.*, **18**(4), 684-695.